Pairing and two-state mixing models in ^{133}Cs

Amir Jalili [1,2,3,*] H. T. Fortune,[4,†] Yan-An Luo,[2] H. Sobhani,[2] Aixi Chen,[1,‡] H. K. Wang,[1] and Feng Pan [5,6]

[1]*Department of Physics, Zhejiang Sci-Tech University, Hangzhou 310018, China*
[2]*School of Physics, Nankai University, Tianjin 300071, People's Republic of China*
[3]*Institute of Theoretical Physics, Faculty of Physics, University of Warsaw, ul. Pasteura 5, PL-02-093 Warsaw, Poland*
[4]*Department of Physics and Astronomy, University of Pennsylvania, Philadelphia, Pennsylvania 19104, USA*
[5]*Department of Physics, Liaoning Normal University, Dalian 116029, People's Republic of China*
[6]*Department of Physics and Astronomy, Louisiana State University, Baton Rouge, Louisiana 70803-4001, USA*

The pairing model with configuration mixing has been applied to the odd-A ^{133}Cs nucleus to study band mixing. Then, a simple two-state mixing model has been utilized for the two lowest ground and excited bands. Unique solutions were identified for the $3/2^+$ and $5/2^+$ mixing in both bands, as well as for the $E2$ matrix elements connecting the basis states. The excited band exhibited greater collectivity compared to the ground-state band. The use of a quasispin pairing operator with configuration mixing significantly improves the model's accuracy, especially in replicating experimental data for positive parity states and $E2$ transition rates.

I. INTRODUCTION

The investigation of odd-mass nuclei has attracted significant interest in nuclear structure studies, particularly with the use of various techniques such as a simple two-state mixing model (TSMM) [1,2] and pairing methods [3,4]. Understanding the coexistence of nuclear states and the mixing between coexisting ground and excited states is essential for exploring nuclear structure phenomena [5]. Since then, numerous advances have been made in the theoretical study of odd-mass nuclei, employing a variety of sophisticated methods. Among these, the algebraic model and the more comprehensive solvable model have emerged as leading frameworks for providing excellent yet straightforward descriptions of the structure of even-even and odd-mass nuclei, respectively [5–7]. These models have achieved significant successes in many cases. However, there are situations where a deeper understanding of other nuclear modalities is needed to clarify the phenomena of mixing and coexistence. For instance, a recent paper by Wu *et al.* introduced a mixing term in the Hamiltonian to achieve optimal results for energy and $E2$ transition rates in even-even nuclei [5]. This approach inspires us to incorporate similar mixing terms in the study of band mixing in odd-A Cs isotope.

In both proton stripping [8,9] and pickup reactions [9] on odd-A nuclei, the cross section for populating vibrational and rotational excited states varies significantly from isotope to isotope. The excitation energy of these excited rotational bands also fluctuates considerably. While these effects are qualitatively understood, quantitative reproduction within a simple model has been challenging. The latest attempt, using the mixing model in even-even nuclei, reproduces trends in transition rates, but detailed studies in odd-A nuclei are still lacking. The aim of the present work is to test the energy spectra and transition rates, and to identify a minimal set of assumptions that produce satisfactory fits to the data. A crucial aspect of studying coexistence phenomena involves examining reactions and determining cross-section ratios to estimate mixing matrix elements between rotational states and normal ground states. Proton-transfer reactions are the best candidate for studying Cs isotopes, as the cross section of these reactions is proportional to the mixing strengths. Although the focus is not on the reaction part, introducing Cs isotopes in the context of $(d, {}^3\text{He})$ and $({}^3\text{He}, d)$ reactions [9] is appropriate for calculating the mixing in odd-mass nuclei.

For the remainder of this paper, we concentrate on ^{133}Cs, which has a wealth of states at low excitation energy—16 excited states below 1.9 MeV [10]. The study of ^{133}Cs has a long history. Thun, *et al.* [11] observed transitions in ^{133}Cs following β^+ decay of ^{133}Ba. They reviewed prior experimental work, and they compared their results with predictions of a simple shell-model calculation [12]. Coulomb excitation with a nitrogen beam provided information on $E2$ strengths [13]. Notea and Gurfinkel [14] obtained additional information concerning branching ratios and transition strengths. Dave *et al.* [15] observed transitions in ^{133}Cs following inelastic neutron scattering. They proposed several new states at low excitation energy. Winn and Sarantites [16] measured directional $\gamma\gamma$ correlations and extracted $E2/M1$ mixing ratios. Kikuchi [17] measured gamma angular distributions in the $(n, n'\gamma)$ reaction and made several spin assignments. Renwick *et al.* [18] observed deexcitation gammas following Coulomb excitation and compared their results with calculations based on an intermediate coupling unified nuclear model [19]. This

*Contact author: jalili@zstu.edu.cn; jalili@nankai.edu.cn
†Deceased.
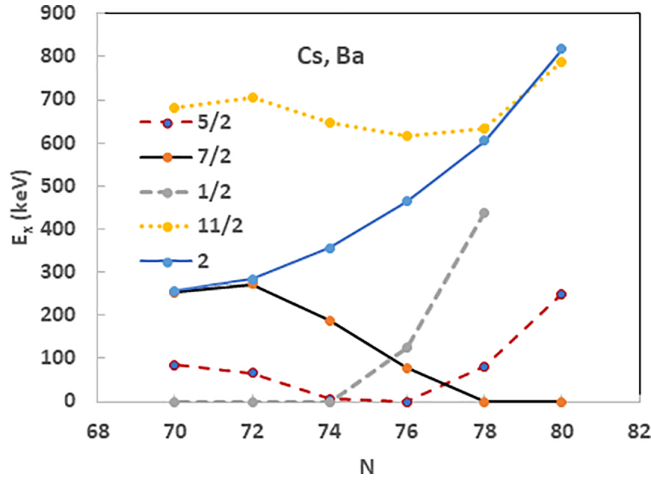‡Contact author: aixichen@zstu.edu.cn

FIG. 1. Energies of selected states in odd-*A* Cs nuclei and the first 2^+ state of even Ba nuclei are plotted vs neuron number.

FIG. 2. Two ratios $R(J, j)$ are plotted vs distance from the closed shell.

calculation produced 27 levels below 1 MeV—several more than are known experimentally. Potnis *et al.* [20] used triple gamma directional correlations to determine additional $E2/M1$ mixing ratios. Teruya *et al.* [21] performed shell-model calculations for several nuclei, including ^{133}Cs. The theoretical orderings of $5/2^+ - 7/2^+$ and $9/2^+ - 11/2^+$ were opposite to the experimental order, but the calculated spacings were small. Biswas *et al.* [22] also performed shell-model calculations, with emphasis on high-*J* states, but they gave orbital decompositions for many states. Nomura *et al.* [23,24] calculated energies and electromagnetic transition strengths for many nuclei, including ^{133}Cs. Theoretical efforts, including shell-model calculations [21,23,24], contribute valuable insights, setting the stage for further exploration of the nuclear structure of ^{133}Cs. For the subsequent discussion, our focus narrows to ^{133}Cs, a nucleus rich in low-excitation states. We will reproduce and discuss their results later based on the mixing Hamiltonian and TSMM configuration. Other experimental work on ^{133}Cs [15,18,19] has focused on high-spin states, which are not relevant for the present paper.

II. THEORETICAL FRAMEWORK

It might be thought reasonable to consider the low-lying states of odd-*A* Cs nuclei as characterized by a proton hole in the ground state (g.s.) and the first 2^+ state of even Ba nuclei. However, the barium nuclei are not well described as a $d_{5/2}$ closed subshell. Results of proton stripping [8,9] and pickup reactions [9] on barium nuclei indicate a substantial vacancy in the $d_{5/2}$ orbital and significant occupancy of the $g_{7/2}$ orbital. This fact is reinforced in Cs nuclei by the presence of more states at low excitation than would be expected from the coupling of a single hole.

Figure 1 displays a plot of the energy of the first 2^+ state of Ba nuclei and energies vs *N* [10] of four states in Cs—having $J^\pi = 5/2^+$, $7/2^+$, $1/2^+$, and $11/2^+$. The lowest $5/2^+$ and $7/2^+$ should have large percentages of single-hole $d_{5/2}$ and $g_{7/2}$, respectively, coupled to Ba g.s. The $1/2^+$ and $11/2^+$ states represent unique couplings of $d_{5/2}$ and $g_{7/2}$,
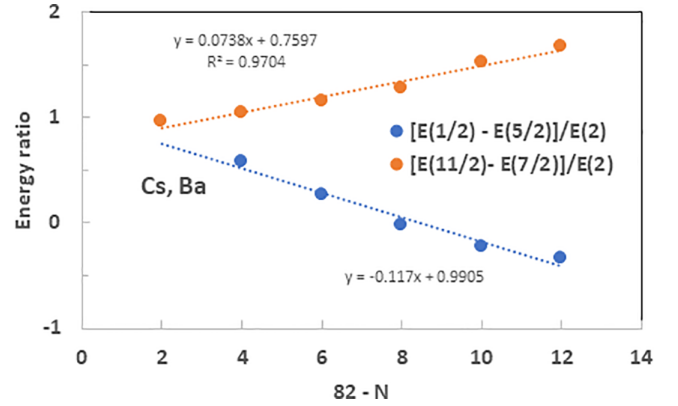
respectively, to the 2^+ of Ba. Note the change in g.s. *J* as one moves along the Cs isotopic chain. No simple features emerge from this plot. We define

$$R(J, j) = [E(J) - -E(j)]/E(2). \tag{1.1}$$

Figure 2 contains a plot of the quantities $[E(1/2) - E(5/2)]/E(2)$ and $[E(11/2) - E(7/2)]/E(2)$. The abscissa is the distance from the neutron major shell closure at $N = 82$. In the limit of extremely weak coupling and in the absence of any residual interaction, both these ratios would be unity. It is gratifying that both tend toward 1 as *N* tends to 82—actually 0.99 for $1/2^+$ and 0.76 for $11/2^+$. The straight lines are the functions $R(J, j) = R_0(J, j) + (a + bJ_c j)(82 - N)$, where $J = J_c + j$, R_0 is the value at $N = 82$, and the dimensionless parameters *a, b* turn out to be $a = -0.0216$, $b = 0.0136$. For *J* between 1/2 and 11/2, there are two states of each *J*, and they can mix, complicating the energies. To clarify the notation used in Eq. (1.1), the ratio between the expectation values, $E(J)$ and $E(j)$, normalized by $E(2)$, signifies the relationship between the two total angular momenta, *J* and *j*. These momenta correspond to the two states for each *J* value (between 1/2 and 11/2) discussed in Fig. 2. As it is clear, in the limit of extremely weak coupling and without residual interaction, this ratio approaches unity for these states near the closed shell ($N = 82$). This highlights the role of the ratio and linear correlation as a signature of the potential for mixing between these states. To investigate this further, we examined various ratios and observed the correlation between the ratio and the deviation from unity in the limit of weak coupling, as shown in the curves. In Fig. 2, for example, one curve represents the case where $J = 1/2$ and $j = 5/2$, and the other curve corresponds to $J = 11/2$ and $j = 7/2$.

While a complete model for the system is not provided at this stage, the observed deviation of the ratio from a linear pattern for certain momenta (Fig. 2) and the rotational linearity suggest a potential influence on the state energies beyond the simple picture of independent states. This linear correlation strongly indicates possible mixing between these rotational states. Further investigation with comprehensive models, such as the TSMM or the mixing configuration Hamiltonian, is

necessary to definitively confirm the nature and extent of this mixing.

A. Solvable pairing model

In this part, we investigate the nuclear structure of the odd-mass nucleus, ^{133}Cs, by employing a theoretical framework based on quasi-spin pairing operators. The study incorporates the pairing model, combining boson and fermion operators to comprehensively describe the nucleus's behavior. The pairing Hamiltonian comprises four components: boson, fermion, their interaction, and a two-configuration mixing term. The model introduces an offset parameter to account for additional particle excitations from the closed shell. The quadrupole, $E2$ operator along with wave functions following $U(5) \supset O(5) \supset O(3)$ symmetry combination with a certain angular momentum $|J_\xi\rangle$ form the basis for calculating energy spectra and transition rates. Results are presented and compared with experimental data, revealing significant insights into the low-lying states of ^{133}Cs.

Now, we introduce the generators of quasispin pairing operators [25–28] with

$$\hat{S}_l^+ = (\hat{S}_l^-)^\dagger = \frac{1}{2} l^\dagger \cdot l^\dagger, \qquad \hat{S}_l^0 = \frac{1}{4} \sum_\mu (l_\mu^\dagger l_\mu + l_\mu l_\mu^\dagger), \quad (1.2)$$

in which $l^\dagger$ and l are the creation and annihilation operators for s and d bosons [29]. By adding single-particle degrees of freedom and using the formalism of second quantization, we introduce the fermion operators

$$a_{j,m}^+, \ (m = \pm 1/2, 3/2, ..., \pm j),$$
$$a_{j,m}, \ (m = \pm 1/2, 3/2, ..., \pm j) \qquad (1.3)$$

in which $a_{j,m}^+$ and $a_{j,m}$ are the creation and annihilation operators for fermion. The operator for the fermion term can be $\hat{q}_F = (a_j^\dagger \times \tilde{a}_j)^{(2)}$. Here, the solvable mixing Hamiltonian used to describe the odd-mass ^{133}Cs nucleus consists of four sections, i.e., the parts that describe the quasispin pairing and phase transition (first and second terms), interaction between boson and fermion (third term), and a two-configuration mixing term (last two terms), the same as in Refs. [6,7]. So, the mixing Hamiltonian $\hat{H}$ is defined as

$$\hat{H} = x\left(\eta \hat{n}_d + \frac{1-\eta}{N} \hat{S}^+ \hat{S}^- - y \frac{2(1-\eta)}{N} \hat{Q}_B \right.$$
$$\left. \cdot \hat{q}_F + g_s(\hat{S}_s^+ + \hat{S}_s^-) + g_d(\hat{S}_d^+ + \hat{S}_d^-) \right), \qquad (1.4)$$

where η is the control parameter. In this Hamiltonian, n_d, N, $\hat{Q}_B$ are the d boson number, total boson number, and quadrupole operators, respectively. The mixing term in the Hamiltonian facilitates band mixing between the ground and certain excited states, as well as the presence of intruder states. However, since this study focuses on band mixing, the intruder states are not a primary concern in this investigation. We introduce the wave function as a linear combination of $U(5) \supset O(5) \supset O(3)$ [30], with a certain angular momentum for the boson-fermion framework

$$|J_\xi\rangle = \sum_{n_d \nu \alpha L} C_{n_d, \nu}^{L, \xi} |N n_d \nu \alpha L; nl j; JM\rangle, \qquad (1.5)$$
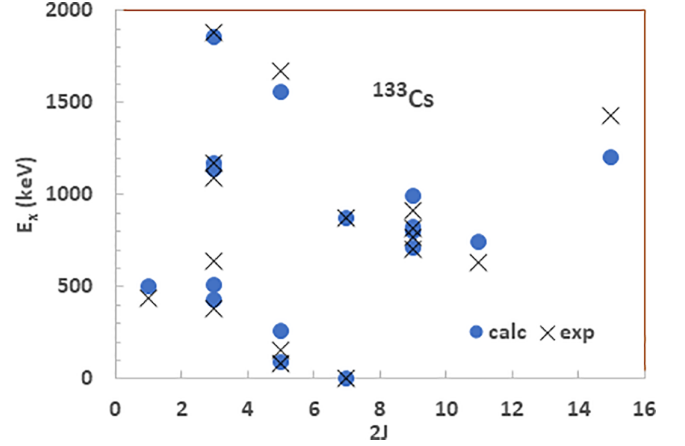

FIG. 3. Level energies for ^{133}Cs. Experimental energies (x) are compared with theoretical level energies (circles) coming from the mixing Hamiltonian based on the mixing configuration. Parameters are taken as $\eta = 0.54$, $g_s = 162$, $g_d = 225$, $x = -0.26$, $y = 1$ in keV. The experimental data are taken from [10].

where $N n_d \nu \alpha L$, $nl j$, J, and M are the total boson number, d boson number, seniority number, an additional quantum number to distinguish different states with the same L, angular momentum, fermion number, orbital quantum number, fermion angular momentum, the total angular momentum quantum number, and third components of the total angular momentum, respectively. Also, the coefficient $C_{n_d, \nu}^{L, \xi}$ is the corresponding amplitude of the eigenvector obtained by diagonalizing the Hamiltonian. These coefficients are prominent in the calculation of $E2$ transition rates. The energy spectra are derived from the diagonalization of the Hamiltonian, with the coefficients x, y, g_s, and g_d serving as fitting parameters. These parameter values are illustrated in Fig. 3. The details of the diagonalization process have been described in our recent papers [4,6,7,28]. In addition to these fitting parameters, the mixing calculation requires another parameter, which we call the offset parameter (Δ) to excite two more particles from the closed shell. The energy spectrum for ^{133}Cs is plotted in Fig. 3. Calculated and experimental energies are compared in this figure.

The quadrupole operator is $\hat{Q}_B = (s^\dagger \times \tilde{d} + d^\dagger \times \tilde{s})^{(2)}$. Also, we have the $E2$ operator as

$$T^{E2} = e^B [s^\dagger \times \tilde{d} + d^\dagger \times \tilde{s}]_\mu^{(2)} + e^F [a_j^\dagger \times \tilde{a}_{j'}]_\mu^{(1)}. \qquad (1.6)$$

We have used the selection rules to obtain the $E2$ transition rates. In these equations, e^B and e^F are the effective charges for the boson and fermion systems, respectively.

B. Band mixing analysis

The simple TSMM, which was previously applied to even-even nuclei exhibiting shape coexistence, focuses on obtaining the most information with the fewest assumptions. Fortune has published many works on band mixing in even-even mass nuclei [31–36]. This approach, unlike most mixing procedures that impose specific structures, remains unbiased and flexible. Recently, Majarshin and Fortune began

TABLE I. Calculated and experimental $E2$ transition strengths (in Weisskopf units) for the positive-parity states in ^{133}Cs. The experimental data are taken from [10].

Label	Initial level		Final level		$B(E2)_{Exp}$	$B(E2)_{Th}$	$B(E2)$
	J_i^π	E (keV)	J_f^π	E (keV)	(W.u.)	(W.u.)	[23]
1	$5/2^+$	80.9979 8	$7/2^+$	0.0	5.8 (4)	6.48	0.49
2	$5/2^+$	160.6121 9	$5/2^+$	80.9979 (8)	130(3)	59.70	0.60
3	$5/2^+$	160.6121 9	$7/2^+$	0.0	28.6 (18)	41.26	23
4	$3/2^+$	383.8491 8	$5/2^+$	160.6121(9)	0.12 (4)	0.23	0.024
5	$3/2^+$	383.8491 8	$5/2^+$	80.9979 (8)	0.04 (+7−4)	0.14	17
6	$3/2^+$	383.8491 8	$7/2^+$	0.0	12 (3)	10.08	1.1
7	$1/2^+$	383.8491 (8)	$3/2^+$	383.8491 (8)	> 18	15.67	8.8
8	$1/2^+$	437.0113 9	5/2	160.6121 (9)	> 4.8	0	0.40
9	$1/2^+$	437.0113 9	$5/2^+$	80.9979 (8)	> 12	0	43
10	$11/2^+$	632.56 10	$7/2^+$	0.0	26.1 (20)	24.55	25
11	$3/2^+$	640.40 7	5/2	160.6121 (9)	3.6 (23)	2.97	2.7
12	$3/2^+$	640.40 7	$5/2^+$	80.9979 (8)	100 (7)	68.77	2
13	$3/2^+$	640.40 7	$7/2^+$	0.0	3.4 (7)	23.69	26
14	$9/2^+$	705.57 9	$5/2^+$	160.6121 (9)	7.0 (17)	27.02	1.8

investigating band mixing in odd-A nuclei [4,28]. Now let us focus on the results of band mixing. The $E2$ strengths linking these states are presented in Tables I and II. Table I specifically shows the results for the transition from $3/2^+$ to $5/2^+$. To aid understanding, we define two bands: the ground (g) and excited (e) states, which are represented by their basis state wave functions. In order to investigate mixing between these states, we write the TSMM,

$$\psi[(3/2)_1] = a\phi[(3/2)_g] + b\phi[(3/2)_e],$$
$$\psi[(3/2)_2] = -b\phi[(3/2)_g] + a\phi[(3/2)_e], \qquad (1.7)$$

$$\psi[(5/2)_1] = c\phi[(5/2)_g] + d\phi[(5/2)_e],$$
$$\psi[(5/2)_2] = -d\phi[(5/2)_g] + c\phi[(5/2)_e], \qquad (1.8)$$

and

$$M_g = \langle(3/2)_g\|M(E2)\|(5/2)_g\rangle,$$
$$M_e = \langle(3/2)_e\|M(E2)\|(5/2)_e\rangle, \qquad (1.9)$$

where, $a^2 + b^2 = c^2 + d^2 = 1$. The simple TSMM is an appropriate model for the first two 0^+ and first two 2^+ states in even-even nuclei, in such a way that each 2^+ basis

state is connected to only one 0^+ basis state by an $E2$ amplitude. We will now extend this model to odd-A nuclei. If one allows a coupling between the two states, the interaction leads to mixed states. Equations (1.7) and (1.8) describe the mixing model, where $\psi(3/2)$ and $\psi(5/2)$ are the perturbed wave functions, and $\Phi(3/2)$ and $\Phi(5/2)$ are defined as the unperturbed wave functions, specifically the $3/2^+$ and $5/2^+$ basis-state wave functions. If we let $\psi(3/2)_1$ and $\psi(3/2)_2$ represent the physical ground state and excited $3/2^+$ state in the nucleus Cs, and $\Phi(3/2)_g$ and $\Phi(3/2)_e$ be the basis levels, then due to the orthonormality in $\Phi(3/2)_g$ and $\Phi(3/2)_e$, we can define the most general TSMM wave function. The calculated $B(E2)$ values provide critical insights into the transition probabilities between nuclear states. To quantify these transitions, we derive matrix elements from the $B(E2)$ values, as shown in Table I. The relationship between the $B(E2)$ values and the matrix elements is detailed in Eq. (1.10), ensuring a clear connection between experimental observations and theoretical calculations. This approach allows for a comprehensive analysis of the mixing configurations in the nuclear states,

$$M(E2) = \sqrt{(2J_i + 1)B(E2; i \rightarrow f)}. \qquad (1.10)$$

TABLE II. Calculated and experimental $E2$ strengths (W.u.) and transition matrix elements [(W.u.)$^{1/2}$] for $3/2^+ \rightarrow 5/2^+$ transitions in ^{133}Cs.

Label	i	f	$B(E2)$ [a]	$M(E2)$ [b]	$B(E2)$, mixing H [c]	$M(E2)$, mixing H
$M0$	$(3/2^+)_1$	$(5/2^+)_1$	$0.04_{(+7-4)}$	$0.16_{(3)}$	0.14	0.74
$M1$	$(3/2^+)_1$	$(5/2^+)_2$	$0.12_{(4)}$	$0.69_{(3.4)}$	0.23	0.95
$M2$	$(3/2^+)_2$	$(5/2^+)_1$	$100_{(7)}$	$\pm20_{(4.5)}$	68.77	16.58
$M3$	$(3/2^+)_2$	$(5/2^+)_2$	$3.6_{(23)}$	$6.45_{(9.5)}$	2.97	3.44

[a] Data taken from Ref. [10].
[b] $M^2(E2) = (2J_i + 1) B(E2; i \rightarrow f)$.
[c] Current work with mixing H.

In line with previous studies [27,37], we assume the g states are not connected to the e states by the $E2$ operator. This simplifies the analysis and allows the properties of the basis states to emerge naturally from the mixing process. The extracted coefficients from $E2$ transitions, governed by the ΔJ selection rule, provide information about the nature of these states without additional assumptions. While we acknowledge that this assumption simplifies the complex nature of $E2$ transitions, it facilitates the analysis without compromising the key findings.

III. RESULTS

Utilizing the wave functions from Eq. (1.4) obtained through the diagonalization of the IBFM mixing Hamiltonian, we calculated $E2$ transitions. The results, detailed in Table. I, are further compared with experimental data as well. For $E2$ transitions, we have employed the fixed values $e^B = 0.22$ and $e^F = 0.51$. $E2$ strengths calculated using the mixing Hamiltonian are presented in Table I. Moreover, relevant $E2$ matrix elements, namely $M(E2)$, derived from both the TSMM and mixing Hamiltonian, are shown in columns 5 and 7, respectively, of Table II. In our study, the simultaneous application of both the solvable model with a mixing term and the TSMM serves complementary purposes. The solvable model aims to understand the effect of the mixing term and to improve the accuracy of the energy spectra and $E2$ transition rates. Previous results have demonstrated that the inclusion of the mixing term enhances the results when both normal and deformed intruder states are present. The TSMM specifically evaluates the strength of mixing between particular states. By using the solvable model with the mixing term, we can identify the states that exhibit mixing potential and accurately determine the $E2$ transition rates. In essence, the solvable model helps us to pinpoint states with significant mixing, while the TSMM provides a detailed understanding of the mixing strength between these states. Together, these models enhance our ability to interpret and predict the nuclear structure and transitions in odd-A nuclei. The inclusion of quasispin pairing operators with mixing configuration significantly improves the model's precision, especially in reproducing experimental data for positive parity states and $E2$ transition rates. This mixing formalism for the pairing model and its results enable us to compute the band mixing in ^{133}Cs. Nomura's work on ^{133}Cs employs a boson-fermion Hamiltonian, comprising three terms: the even-even boson core or interacting boson Hamiltonian H_B, the single-particle Hamiltonian for unpaired fermions H_F, and the boson-fermion coupling term H_{BF}. The exchange Hamiltonian encompasses dynamical quadrupole, exchange, and monopole interactions. In Fig. 20 of Ref. [23], positive- and negative-parity excitation spectra for ^{133}Cs reveal low-energy structures primarily described by $1g_{7/2}$ and $2d_{5/2}$ (for positive parity) and $1h_{11/2}$ (for negative parity) orbitals weakly coupled to corresponding boson states. These spectra, obtained through the diagonalization of the boson-fermion Hamiltonian, exhibit reasonable agreement with experimental data. Acknowledging the unique couplings of $d_{5/2}$ and $g_{7/2}$ in $1/2^+$ and $11/2^+$ states, leading to band mixing and complicating the energies, our study

successfully reproduces the data by incorporating a two-mixing configuration scheme into the Hamiltonian.

In comparison with the exact solution and the mixing configuration scheme, our study exhibits a reasonably good agreement, further validating the efficacy of the proposed approach in reconciling the experimental observations. The calculated $B(E2)$ transition rates, presented in Tables I and II (compared to Table VIII of Ref. [23]), align well with experimental data. Notably, favorable outcomes are observed for transitions such as $B(E2; \rightarrow (5/2)_1^+ \rightarrow (7/2)_1^+)$ and $B(E2; \rightarrow (3/2)_1^+ \rightarrow (7/2)_1^+)$, with recorded values of 6.53 and 11.13, respectively. These results stand in contrast to major discrepancies found when comparing with Nomura's model, particularly for transitions involving $B(E2; \rightarrow (3/2)_1^+ \rightarrow (5/2)_2^+)$ and $B(E2; \rightarrow (3/2)_2^+ \rightarrow (7/2)_1^+)$. The observed disparities between our work and Nomura's results may be attributed to less collective behavior and can be traced back to the structure of the boson-fermion wave functions. Consequently, our solvable model, incorporating a mixing configuration, provides reasonable agreement with available experimental data for low-energy positive parity states and electromagnetic transition rates in ^{133}Cs. The interacting boson-fermion model based on the Gogny energy density functional, as well as the discrepancies observed with Nomura's work, highlight the effectiveness of the proposed approach. Notably, the incorporation of quasispin pairing operators with a mixing configuration enhances the model's accuracy, particularly in reproducing experimental data for positive parity states and $E2$ transition rates. Using the mixing formalism for the pairing model and its outcomes, we can effectively analyze band mixing in ^{133}Cs.

Now let us focus on the results of band mixing. The $E2$ strengths connecting the basis states are presented in Tables I and II. Table I specifically shows the results for the transition $3/2^+ \rightarrow 5/2^+$. When we apply the equation $M^2(E2) = (2J_i + 1)B(E2; i \rightarrow f)$ to obtain the $E2$ transition matrix elements, the signs of some of the M values can be ambiguous if only the $B(E2)$ values are known. However, the fitting procedure may help in determining these signs. The $E2$ transition matrix elements connecting the relevant states are listed and labeled as $M0$, $M1$, $M2$, and $M3$, as indicated in the first column of Table I. For instance, we define $M0 = acM_g + bdM_e$. In the context of ^{133}Cs, band mixing is suspected in the low-lying states. A simple TSMM has been shown to provide a good description of the $B(E2)$ strengths without any initial assumptions about the structure of the basis states. The properties of these states emerge as a result of the analysis. Consider the $E2$ transition matrix elements connecting the $(3/2)^+$ and $(5/2)^+$ states. If all four of these matrix elements are known, a fit using this simple model can yield the wave-function mixing amplitudes for the $(3/2)^+$ and $(5/2)^+$ states, as well as numerical values of the $M(E2)$ matrix elements connecting the basis states. The fit reproduces the central values of the experimental matrix elements, thereby confirming the effectiveness of the TSMM in describing the mixing and transition rates. It is straightforward to formulate equations for the $E2$ transition matrix elements, such as $M0 = acM_g + bdM_e$, and similarly for other transitions.

TABLE III. Results of TSMM and mixing H for $3/2^+ \leftrightarrow 5/2^+$ transitions in ^{133}Cs.

Quantity	Value (fit 1-TSMM)	Value (fit 2-TSMM)	Value (mixing H)
b	0.033	0.028	0.054
d	0.107	0.105	0.205
M_g	0.133 (W.u.)$^{1/2}$	0.181 (W.u.)$^{1/2}$	0.778 (W.u.)$^{1/2}$
M_e	6.43 (W.u.)$^{1/2}$	6.48 (W.u.)$^{1/2}$	16.9 (W.u.)$^{1/2}$

When calculating $M(E2)$ from $B(E2)$ for connecting the basis states, sign ambiguities can occur when taking square roots, which may lead to destructive interference in $M1$ and $M2$ transitions. In our phase convention, $M0$ and $M3$ are positive, while $M1$ and $M2$ can have either sign. In the current study, the fitting procedure allows both signs for $M2$. With all four relevant matrix elements available, the four parameters (two mixing amplitudes, M_g and M_e) can be uniquely determined. The outcomes of this procedure for ^{133}Cs are presented in Table III. We found one solution with $b = 0.033$, $d = 0.107$, $M_g = 0.133$ (W.u.)$^{(1/2)}$, and $M_e = 6.43$ (W.u.)$^{(1/2)}$, and another with $b = 0.028$, $d = 0.105$, $M_g = 0.181$ (W.u.)$^{(1/2)}$, and $M_e = 6.48$ (W.u.)$^{(1/2)}$. The simple mixing model reveals that the excited bands are 48 times more collective than the ground bands, whereas, according to the band mixing formalism in the mixing Hamiltonian, the collectivity is 20 times greater in excited bands than ground bands. This suggests that the results obtained using the IBFM confirm the pattern of band mixing in the Cs isotope.

The findings suggest that the first $3/2^+$ state is predominantly part of the g band, while the first $5/2^+$ state is primarily associated with the excited e band. Calculations of the basis state energies using these amplitudes yield the values presented in Table I. The mixing matrix elements M_g and M_e are proportional to the transition rates, allowing us to assess the collectivity of the bands. The observed total strength of the $E2$ for the e band is significantly higher compared to the g band. This suggests that the e band is associated with a higher level of collectivity and/or deformation. This analysis allows us to deduce the degree of collectivity within the system. So, the total M_g for the e band is greater than for the g band, suggesting a significant degree of collectivity between the $3/2^+$ and $5/2^+$ states.

IV. CONCLUSION

In summary, our investigation of the nuclear structure of ^{133}Cs using a solvable mixing Hamiltonian based on quasispin pairing operators has provided valuable insights into band mixing in odd-A systems. By accounting for both the even-even boson core and unpaired fermions, the theoretical framework offers a comprehensive understanding of the nucleus. The simple TSMM and the mixing Hamiltonian revealed that the excited bands are more collective compared to the ground bands. The compatibility and discrepancies with other studies highlight the significant role of the mixing configuration in refining the model's accuracy. Our study advances the understanding of odd-mass nuclei by confirming the results of the TSMM through the mixing Hamiltonian, demonstrating the occurrence of band mixing in ^{133}Cs. This work underscores the robustness of the proposed theoretical model in describing the intricate features of low-lying states and $E2$ transition rates in ^{133}Cs. The knowledge gained from this study includes the following: (i) Enhanced understanding of band mixing: We confirmed that the mixing Hamiltonian significantly improves the accuracy of predicting experimental data for positive parity states and $E2$ transition rates. (ii) Collectivity analysis: The analysis of $E2$ strengths indicated that the excited bands possess greater collectivity and deformation compared to the ground bands. (iii) Validation of theoretical models: Our results validate the use of quasispin pairing operators and the TSMM in analyzing band mixing, providing a reliable method for future studies on odd-mass nuclei.

Future studies can build on this work by applying the mixing Hamiltonian approach to other odd-mass nuclei, exploring the impact of different configurations, and investigating additional transition rates to further refine and validate the theoretical models.

[1] M. Carchidi, H. T. Fortune, G. S. F. Stephans, and L. C. Bland, Phys. Rev. C **30**, 1293 (1984).

[2] M. Carchidi and H. T. Fortune, Phys. Rev. C **38**, 1403 (1988).

[3] F. Pan, Y. Zhang, L. Dai, J. P. Draayer, and D. Kekejian, Phys. Lett. B **848**, 138340 (2024).

[4] A. J. Majarshin, Y.-A. Luo, F. Pan, and H. T. Fortune, Phys. Rev. C **104**, 014321 (2021).

[5] Y. Wu, X. Qi, F. Pan, and J. P. Draayer, Phys. Rev. C **109**, 044310 (2024).

[6] F. Pan, D. Li, G. Cheng, Z. Qiao, J. Bai, and J. P. Draayer, Phys. Rev. C **97**, 034316 (2018).

[7] F. Pan, S. Yuan, Z. Qiao, J. Bai, Y. Zhang, and J. P. Draayer, Phys. Rev. C **97**, 034326 (2018).

[8] K. Nakai, P. Kleinheinz, J. Leigh, K. Maier, F. Stephens, R. Diamond, and G. Løvhøiden, Phys. Lett. B **44**, 443 (1973).

[9] B. Wildenthal, E. Newman, and R. Auble, Phys. Rev. C **3**, 1199 (1971).

[10] Y. Khazov, A. Rodionov, and F. G. Kondev, Nucl. Data Sheets **112**, 855 (2011).

[11] J. Thun, S. Törnkvist, K. B. Nielsen, H. Snellman, F. Falk, and A. Mocoroa, Nucl. Phys. **88**, 289 (1966).

[12] L. S. Kisslinger and R. A. Sorensen, Rev. Mod. Phys. **35**, 853 (1963).

[13] N. Imanishi, F. Fukuzawa, M. Sakisaka, and Y. Uemura, Nucl. Phys. A **101**, 654 (1967).

[14] A. Notea and Y. Gurfinkel, Nucl. Phys. A **107**, 193 (1968).

[15] V. Dave, J. Nelson, and R. Wilenzick, Nucl. Phys. A **142**, 619 (1970).

[16] W. Winn and D. Sarantites, Phys. Rev. C **1**, 215 (1970).

[17] K. Shiroh, Nucl. Phys. A **171**, 480 (1971).

[18] B. Renwick, B. Byrne, D. Eastham, P. Forsyth, and D. Martin, Nucl. Phys. A **208**, 574 (1973).

[19] D. Choudhury and J. Friedman, Phys. Rev. C **3**, 1619 (1971).

[20] V. Potnis, G. Agin, and B. Singh, Nucl. Phys. A **436**, 93 (1985).

[21] E. Teruya, N. Yoshinaga, K. Higashiyama, and A. Odahara, Phys. Rev. C **92**, 034320 (2015).

[22] S. Biswas *et al.*, Phys. Rev. C **95**, 064320 (2017).

[23] K. Nomura, R. Rodríguez-Guzmán, and L. M. Robledo, Phys. Rev. C **96**, 064316 (2017).

[24] K. Nomura, T. Nikšić, and D. Vretenar, Phys. Rev. C **96**, 014304 (2017).

[25] F. Pan and J. Draayer, Nucl. Phys. A **636**, 156 (1998).

[26] F. Pan, Y. Zhang, H.-C. Xu, L.-R. Dai, and J. P. Draayer, Phys. Rev. C **91**, 034305 (2015).

[27] A. J. Majarshin, Y.-A. Luo, F. Pan, H. T. Fortune, and J. P. Draayer, Phys. Rev. C **103**, 024317 (2021).

[28] A. Majarshin, Y.-A. Luo, F. Pan, H. Fortune, Y. Zhang, and J. Draayer, J. Phys. G: Nucl. Part. Phys. **48**, 125107 (2021).

[29] A. J. Majarshin, Eur. Phys. J. A **54**, 11 (2018).

[30] A. J. Majarshin and M. A. Jafarizadeh, Nucl. Phys. A **968**, 287 (2017).

[31] H. T. Fortune, Phys. Rev. C **94**, 024318 (2016).

[32] H. T. Fortune, Phys. Rev. C **98**, 064303 (2018).

[33] H. T. Fortune, Phys. Rev. C **99**, 054320 (2019).

[34] H. T. Fortune, Phys. Rev. C **100**, 044303 (2019).

[35] H. Fortune, Nucl. Phys. A **1014**, 122233 (2021).

[36] H. T. Fortune, Phys. Rev. C **105**, 014324 (2022).

[37] A. J. Majarshin, Y.-A. Luo, F. Pan, and J. P. Draayer, Chin. Phys. C **45**, 024103 (2021).